2012

Interface dipole effect on thin film ferroelectric stability: First-principles and phenomenological modeling

Xiaohui Liu
University of Nebraska-Lincoln, phyliuxiaohui@gmail.com

Yong Wang
University of Nebraska-Lincoln, ywang@cse.unl.edu

Pavel V. Lukashev
University of Nebraska-Lincoln, pavel.lukashev@uni.edu

John D. Burton
University of Nebraska-Lincoln, jburton2@unl.edu

Evgeny Y. Tsymbal
University of Nebraska-Lincoln, tsymbal@unl.edu

Interface dipole effect on thin film ferroelectric stability: First-principles and phenomenological modeling

Xiaohui Liu, Yong Wang, Pavel V. Lukashev, J. D. Burton,[*] and Evgeny Y. Tsymbal[†]

Department of Physics and Astronomy, Nebraska Center for Materials and Nanoscience, University of Nebraska, Lincoln, Nebraska 68588-0299, USA

Utilization of the switchable spontaneous polarization of ferroelectric materials offers a promising avenue for the future of nanoelectronic memories and logic devices provided that nanoscale metal-ferroelectric-metal heterostructures can be engineered to maintain a bi-stable polarization switchable by an applied electric field. The most challenging aspect of this approach is to overcome the deleterious interface effects which tend to render ferroelectric polarization either unstable or unswitchable and which become ever more important as ferroelectric materials are produced thinner and thinner. Here we use first-principles density functional calculations and phenomenological modeling to demonstrate that a BaO/RuO_2 interface termination sequence in $SrRuO_3/BaTiO_3/SrRuO_3$ epitaxial heterostructures grown on $SrTiO_3$ can lead to a nonswitchable polarization state for thin $BaTiO_3$ films due to a fixed interface dipole. The unfavorable interface dipole at the BaO/RuO_2 interface leads to a strong preference for one polarization state and, in thin film structures, leads to instability of the second state below a certain critical thickness, thereby making the polarization unswitchable. We analyze the contribution of this interface dipole to the energetic stability of these heterostructures. Furthermore, we propose and demonstrate that this unfavorable interface dipole effect can be alleviated by deposition of a thin layer of $SrTiO_3$ at the BaO/RuO_2 terminated interface. Our first-principles and phenomenological modeling predict that the associated change of the interface termination sequence to SrO/TiO_2 on both sides of the heterostructure leads to a restoration of bi-stability with a smaller critical thickness, along with an enhancement of the barrier for polarization reversal. These results demonstrate that interface engineering is a viable approach to enhance ferroelectric properties at the nanoscale.

　　　　　　　　　　PACS number(s): 77.80.bn, 77.55.fe, 77.55.Px

I. INTRODUCTION

Ferroelectric materials are promising for a variety of technological applications such as nonvolatile random access memories and high-density data storage devices.[1] This is due to their spontaneous polarization which can be switched between two (or more) stable polarization states and thus can be used as a memory state variable. Continuing demand to further miniaturize electronic devices brings up a problem of ferroelectric polarization stability at the nanometer scale.[2,3] In particular, one of the promising research directions involve ferroelectric tunnel junctions,[4–6] which rely on the existence of polarization in the ferroelectric barrier layers with thicknesses of just several unit cells. Switchable polarization of the tunnelling barrier allows for a giant change in resistance in such junctions, known as the tunneling electroresistance effect,[7,8] and control of the transport spin polarization if the electrodes are ferromagnetic.[9–14] Thus, maintaining and controlling a stable and switchable electric polarization in ferroelectric thin films down to the nanometer thickness range at room temperature is essential for exploiting the functionality of these materials for nanoelectronics applications.

In thin film structures with perpendicular-to-the-plane ferroelectric polarization the polarization charges accumulated on the two surfaces of the film produce a depolarizing field. This depolarizing field is largely responsible for determining thin film ferroelectric stability. The depolarizing field can be reduced by formation of screening charges at the film-electrode interfaces[15–17] and/or by forming a non-uniform domain structure.[18–24] In some cases, however, the screening provided by conductive electrodes in metal-ferroelectric-metal structures appears to be insufficient, resulting in unstable ferroelectric polarization. For example, it was found that high-quality ultrathin $SrRuO_3/BaTiO_3/SrRuO_3$ capacitors exhibit severe relaxation of $BaTiO_3$ polarization within a few microseconds.[25] This effect is a consequence of strong effective depolarizing fields due to incomplete screening or the reduced interface capacitance effect.[26] These effects can smear out the ferroelectric phase transition and make ferroelectricity unstable at room temperature. In addition, the presence of asymmetric interfaces may lead to a built-in electric field whose direction is independent of polarization orientation, resulting in two non-equivalent polarization states.[27] In fact such asymmetry may even destroy the stability of one of the polarization states, making the system only monostable in zero applied field and therefore nonferroelectric.[28] Addressing these detrimental effects is critical both for the fundamental understanding of the ferroelectric behavior at the nanoscale and related device performances.

Recently, first-principles calculations have predicted that interface atomic structure and chemical bonding at the interface may significantly impact a thin film ferroelectric state.[29] The local chemical environment at the interfaces affects thin film ferroelectricity through the electrode-oxide bonds, which may enhance or reduce ferroelectric displacements. In particular, it was found that interfaces formed between AO-terminated perovskites and simple metals may produce interfacial ferroelectricity, which enhances ferroelectricity of the whole film.[30] These findings open an efficient way to

stabilize and even enhance ferroelectricity in nm-thick films through interface engineering.

In this work we exploit this approach to enhance ferroelectricity in thin $BaTiO_3$ films sandwiched between two $SrRuO_3$ electrodes. Using first-principles calculations and phenomenological modeling we demonstrate that introduction of a very thin layer of $SrTiO_3$ at the $BaTiO_3$/$SrRuO_3$ interface eliminates an unfavorable built-in electrostatic dipole at BaO/RuO_2 terminated interfaces, leading to smaller critical thickness for a stable and switchable ferroelectric polarization even at room temperature. Our theoretical predictions have recently been confirmed by the experiment.[31]

II. FIRST PRINCIPLES CALCULATIONS

A. Method

Density functional theory calculations of atomic and electronic structures are performed using the plane-wave projector-augmented-wave (PAW) method implemented in the Vienna *Ab Initio* Simulation Package (VASP).[32] A plane-wave cutoff energy of 500 eV and the local density approximation (LDA) for the exchange and correlation functional were used in all calculations. Atomic relaxations were converged using an $8 \times 8 \times 1$ Monkhorst-Pack k-point sampling of the Brillouin zone until forces were less than 20 meV/Å.

B. Structures

We study a series of several related heterostructure supercells of the form $[SrRuO_3]_4/[BaTiO_3]_n/[SrRuO_3]_4$ or $[SrRuO_3]_4/[BaTiO_3]_n[SrTiO_3]_m/[SrRuO_3]_4$ with $n = 8$, 6, 5, 4 and $m = 1$, 2. $SrTiO_3$, $BaTiO_3$, and $SrRuO_3$ belong to the same pseudocubic perovskite-oxide family with formula unit ABO_3. To simulate coherent epitaxial growth on a (001) oriented substrate of $SrTiO_3$ we constrain the in-plane structure of each bulk material component of the heterostructure to a 1×1 cubic perovskite cell with lattice constant $a = 3.871$Å consistent with the calculated LDA lattice constant of cubic $SrTiO_3$ and perform full relaxation of the internal z-coordinates and tetragonal out-of-plane lattice constant c. For the metallic $SrRuO_3$ we find a centrosymmetric tetragonal structure with $c/a = 1.013$, and for ferroelectric $BaTiO_3$ we find a polar structure consistent with previous calculations and c/a ratio 1.055. For $SrTiO_3$ the structure remains cubic with $c/a = 1$. The supercells are then constructed by stacking these structural unit cells along the [001] direction (which we consider the z-axis) and performing full internal relaxation and overall c/a ratio of the supercell subject to the same in-plane constraint. Figures 1(a) and 2(a) show schematic side views of the $SrRuO_3$/$[BaTiO_3]_8$/$SrRuO_3$ and $SrRuO_3$/$[BaTiO_3]_6[SrTiO_3]_2$/$SrRuO_3$ supercells, respectively. Due to computational limitations we ignore the antiferrodistortive tilts and rotations of the oxygen octahedra, which are known to occur in some perovskite oxides,[33] which would require a doubling of the in-plane size of the cell and therefore double the number of atoms in the system. These octahedral distortions occur at low temperatures and suppressing them, as has been done in other first-principles studies,[34,35] should not appreciably affect the stability of ferroelectricity in $BaTiO_3$.
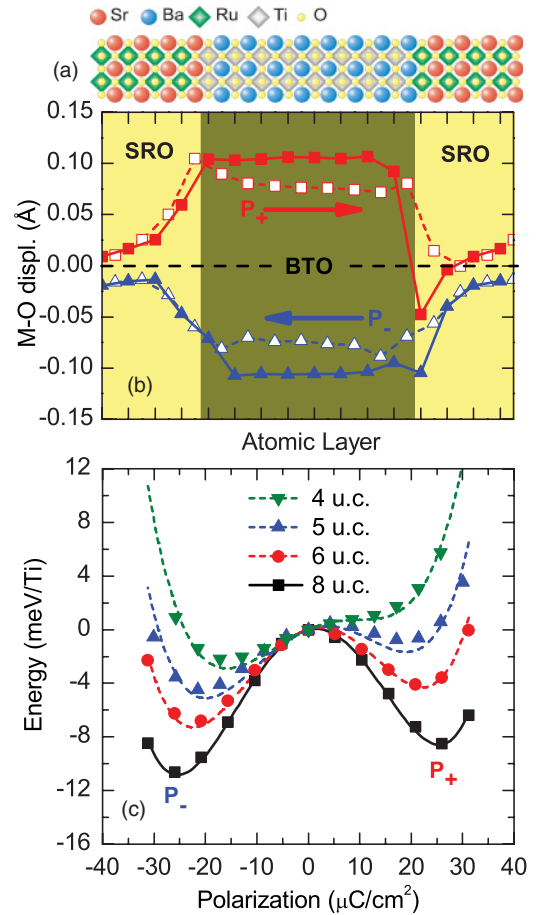

FIG. 1. (Color online) (a) Atomic structure of the $SrRuO_3$/$[BaTiO_3]_8$/$SrRuO_3$ supercell with the BaO-RuO_2 termination at the top (right) interface. (b) Layer-by-layer profile of the polar metal-oxygen (M-O) relative z-displacements for the two polarization states. Squares and triangles correspond to the P_+ and P_- states, respectively. Open symbols correspond to Ba-O and Sr-O displacements; closed symbols correspond to Ti-O_2 and Ru-O_2 displacements, respectively. (c) Total energy per Ti atom calculated form first-principles (symbols) and phenomenological modeling (curves) as a function of z-averaged polarization of $BaTiO_3$ for $SrRuO_3$/$[BaTiO_3]_n$/$SrRuO_3$ heterostructures with different number of $BaTiO_3$ unit cells: $n = 8$, 6, 5, and 4 (squares, circles, up-triangles, down-triangles). The solid curve for $n = 8$ is a fit to the phenomenological model (see Sec. III). The dashed curves for the thinner structures use the thickness-independent fitting parameters derived from $n = 8$ fit.

C. Polarization stability of $SrRuO_3$/$[BaTiO_3]_n$/$SrRuO_3$

The presence or absence of two different stable polarization states in each of the asymmetric $SrRuO_3$/$[BaTiO_3]_n$/$SrRuO_3$ heterostructures with $n = 8$, 6, 5, or 4 is tested by careful construction of the initial (prerelaxation) supercell. During the first step of constructing each supercell the $BaTiO_3$ is assumed to have only a small deviation from its nonpolar centrosymmetric state, i.e., with small relative displacement of Ti and Ba atoms with respect to their in-plane oxygen neighbors either along $+z$ or $-z$. The polarization state with polarization pointing away from the BaO/RuO_2 interface was easily established for all $BaTiO_3$ thicknesses tested. In this

case the polarization is pointing along $-z$, and we denote this state as the P_- state. For the opposite polarization state in these structures, however, this procedure did not always lead to a stable polarization. In this case the polarization is pointing along $+z$, and we denote this state as the P_+ state. In the $n = 8$ structure both polarization states are stabilized, as can be seen from the layer-by-layer metal-oxygen relative z-displacements in Fig. 1(b). The $n = 6$, 5, and 4 structures, however, always relaxed to the opposite, P_- state. In these cases exhaustive tests were performed with different starting polarization structures in an attempt to find a stable P_+ state, but to no avail. This indicates that the $n = 6$, 5, and 4 structures are only mono-stable, with polarization pointing away from the BaO/RuO$_2$ interface.

The origin of this preference for the P_- state can be discerned by examination of the metal-oxygen displacements of the $n = 8$ structure shown in Fig. 1(b). The first point to notice is that the Ba-O and Ti-O$_2$ relative displacements all maintain the same sign and roughly the same magnitude throughout the BaTiO$_3$ layer, indicating that the ferroelectric polarization is more or less uniform. Second, we note that there are also Sr-O and Ru-O$_2$ displacements whose magnitude decay away from the interfaces into the bulk of the SrRuO$_3$ metallic electrode. For the most part these polar displacements in the SrRuO$_3$ follow the ferroelectric polarization in the BaTiO$_3$. This follows from the fact that the electrodes possess a finite screening length, and electric fields can penetrate them to cause an ionic polar response of the structure. This effect plays an integral role in the electrostatic properties of heterostructures containing metallic oxides and has been studied both theoretically[26,36] and experimentally[37] in different materials systems. The exception in our case, however, appears to be at the BaO/RuO$_2$ terminated interface for the P_+ state where the polar displacements in the first two RuO$_2$ layers of the electrode are opposite to the ferroelectric polarization. The signature of this built-in distortion at the BaO/RuO$_2$ interface also appears in the P_- state as an enhanced negative polar displacement on the first interface RuO$_2$ layer in Fig. 1(b).

The interface dipole arises due to a mismatch between ionic radii: the Sr-Ti interface can be viewed as one cell of SrTiO$_3$, whose cationic radii complement one another so that it has a preference to be centrosymmetric, and will therefore only develop off-centering in response to an electric field. At the Ba-Ru interface, however, Ba has a larger ionic radius than Sr and, just as it does in BaTiO$_3$, leads to off-centering of the B-site cation (Ru^{4+} in this case) with respect to the co-planar oxygen ions. The asymmetric environment of the interfacial Ru, however, strongly favors only one orientation (negative in our case). In addition, BaRuO$_3$, which is essentially what we have at the Ba-Ru interface, only assumes the pseudo-cubic-perovskite structure similar to SrRuO$_3$ at high pressures due to the larger A-site cationic radius.[38] The presence of a built-in interface dipole at the BaTiO$_3$/SrRuO$_3$ interface with this termination has been noted in previous works.[10,34] We note, however, that this dipole forms due to fixed interface displacements and hence has a different origin compared to the charge-mismatch effect[37] or the effect of a polar interface.[39]

The question remains as to what role, if any, this built-in dipole affects the polarization stability. First, we note that the

two polarization states in the $n = 8$ structure differ in energy by $E_+ - E_- = 2.15$ meV/Ti, where $E_\pm$ is the energy of the $P_\pm$ state. In addition, the polar displacements in the BaTiO$_3$ are slightly larger for the P_- state than for the P_+ state. Both are consistent with the idea of a built-in electrostatic interface dipole pointing in the $-z$ direction.

To gain a more comprehensive, though only semiquantitative, picture of the interface dipole effect on polarization stability, we perform a series of calculations which interpolate between these two polarized states. The two polarization states differ only in the atomic z-positions, with atom m having z coordinate $z_m{}^\pm$ in the $P_\pm$ state. Using these positions we construct a series of structures parameterized by the dimensionless constant λ with z-coordinates

$$z_m(\lambda) = (1 - \lambda)z_m^+ + \lambda z_m^- \qquad (1)$$

and perform fully self-consistent calculations to obtain the energy of each structure, $E(\lambda)$. To obtain the energy vs polarization we estimate the local polarization distribution within BaTiO$_3$ using a model based on the Born effective charges[40] by computing the local polarization $P(z)$ in the BaTiO$_3$ as follows:[41]

$$P(z) = \frac{e}{\Omega} \sum_{m=1}^{N} Z_m^* \delta z_m. \qquad (2)$$

Here N is the number of atoms in the primitive unit cell, δz_m is the displacement of the mth atom away from its position in the centrosymmetric structure, and Ω is the volume of the unit cell. The Born effective charges Z_m^* are 2.77 and 7.25 for Ba and Ti, respectively, and -2.15 and -5.71 for O ions in the TiO$_2$ and BaO planes, respectively.[42] Using these values the polarization of the strained bulk BaTiO$_3$ is calculated to be 27 μC/cm^2, which is in excellent agreement with our calculated value of 26 μC/cm^2 based on the first-principles Berry phase method.[43]

For the supercell heterostructure we then average this $P(z)$ over the BaTiO$_3$ layer for each intermediate scaled structure to obtain $P(\lambda)$ and therefore $E(P)$, which is plotted as squares for the $n = 8$ case in Fig. 1(c). [The curves in Fig. 1(c) correspond to the zero-temperature phenomenological modeling discussed in Sec. III below.] It is seen that this double-well potential is asymmetric due to the presence of the built-in interface dipole. The two minima correspond to the two stable polarization states, and the well depth with respect to $P = 0$ for each minimum corresponds to an effective barrier for polarization reversal. This barrier height, however, only corresponds to a very restricted path through the dense structural phase space for polarization reversal defined by Eq. (1). Instead we can view these barrier heights as an upper bound on the minimum energy required for switching in real systems where reversal can occur through a myriad of other routes, e.g., here we only consider a path where polarization remains more or less uniform throughout the BaTiO$_3$ during reversal, whereas, in reality, developing a non-uniform polarization may significantly lower the barrier. Nevertheless, this energy profile provides clear insight into how the interface dipole affects polarization stability.

We use the same procedure to explore the energetics of the $n = 6$, 5, and 4 structures, which are also plotted in Fig. 1(c). For these structures, however, a stable P_+ state does not exist,

and we use an artificial procedure to construct a state with which to compare the P_- state. This is done by taking the stable P_+ structure from the $n = 8$ heterojunction, removing 2, 3, and 4 BaTiO$_3$ unitcells from the center and rigidly shifting the atomic positions to form a continuous structure corresponding to the average c/a ratio for BaTiO$_3$. With this artificial P_+ state for the thinner structures we then perform the procedure based upon Eqs. (1) and (2) for scaling between the two states and then construct the energy profiles shown in Fig. 1(c).

Again we find an asymmetric energy vs polarization profile for each heterojunction. The $n = 4$ structure shows no minima for a P_+ state. For the $n = 6$ and 5 systems, however, we find an apparent P_+ minimum along this parameterized reversal path. These minima should be viewed with caution: they do not correspond to true metastable energetic minima but instead correspond to projections of unstable saddle-points in the phase space of possible structures. Nevertheless, it is clear that the asymmetry induced by the interface provides a significant contribution to the destabilization of switchable ferroelectricity in these junctions as BaTiO$_3$ thickness decreases.

It is known that the depolarizing effects due to the incomplete screening of bound polarization charges at the interface between the ferroelectric and a metal electrode can lead to the suppression of stable polarization.[25] This effect, however, is expected to destroy polarization *symmetrically* in ferroelectric capacitors with identical electrode materials, i.e., it will decrease the well depth of both polarization states and therefore lead to the absence of both polarization minima below a critical thickness. This effect is certainly present in our system, as can be seen by the systematic decrease in well depth as thickness decreases [see Fig. 1(c)]. In our case, however, the presence of a stable P_- state indicates that the interface dipole effect suppresses the useful switchability of each structure at a higher critical thickness than the one associated with incompletely screened depolarization fields, which would destabilize the P_- state as well.

D. Polarization stability of SrRuO$_3$/[BaTiO$_3$]$_{n-2}$[SrTiO$_3$]$_2$/SrRuO$_3$

The results reported above provide clear evidence of the detrimental effect of the RuO$_2$/BaO termination on the formation of switchable ferroelectric polarization in SrRuO$_3$/[BaTiO$_3$]$_n$/SrRuO$_3$ heterostructures. To alleviate this effect, a natural course of action is to eliminate the detrimental BaO/RuO$_2$ termination in favor of the apparently more stabilizing TiO$_2$/SrO interface. This may be achieved by depositing a thin SrTiO$_3$ interlayer at the BaO/RuO$_2$ terminated interface. Below we focus on a two unit-cell SrTiO$_3$ layer between the BaTiO$_3$ and SrRuO$_3$ electrodes, as shown in Fig. 2(a).

Calculations of the SrRuO$_3$/[BaTiO$_3$]$_{n-2}$[SrTiO$_3$]$_2$/SrRuO$_3$ structures confirm the stabilizing nature of the SrTiO$_3$ interlayer. In particular, we find that the $P_\pm$ states are nearly degenerate for the $n = 8$, 6, 5 "interface engineered" structures. The layer-by-layer atomic metal-oxygen relative displacements for the $n = 8$ structure are plotted in Fig. 2(b). In contrast to the pure BaTiO$_3$ system [Fig. 1(b)], we find that the sign of the polar displacements in every layer (including in the SrTiO$_3$ and SrRuO$_3$) follows the ferroelectric polarization of the BaTiO$_3$ layer, indicating that there are no detrimental
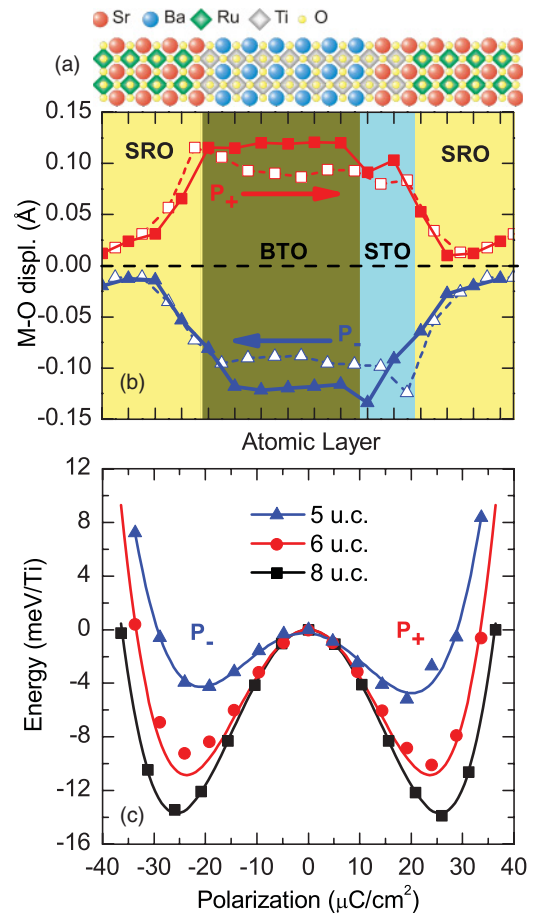

FIG. 2. (Color online) (a) Atomic structure of the SrRuO$_3$/[BaTiO$_3$]$_6$[SrTiO$_3$]$_2$/SrRuO$_3$ supercell with the SrTiO$_3$ additional layer at the top (right) interface. (b) Layer-by-layer profile of the polar metal-oxygen (M-O) relative $z-$displacements for the two polarization states. Squares and triangles correspond to the P_+ and P_- states, respectively. Open symbols correspond to Ba-O and Sr-O displacements; closed symbols correspond to Ti-O$_2$ and Ru-O$_2$ displacements. (c) Total energy per Ti atom calculated form first-principles (symbols) and phenomenological modeling (curves) as a function of z-averaged polarization of BaTiO$_3$ for SrRuO$_3$/[BaTiO$_3$]$_{n-2}$[SrTiO$_3$]$_2$/SrRuO$_3$ heterostructures with different number of BaTiO$_3$ unit cells: $n = 8$, 6, and 5 (squares, circles, up-triangles, down-triangles).

built-in interface dipoles that oppose polarization stability in either polarization state.

Following the same procedure as in Sec. II.C, we calculate the energy profiles for each junction. As seen from Fig. 2(c), all the energy profiles consist of a nearly symmetric double-well, with each corresponding to a stable polarization state. In addition to the recovered switchability of these junctions, we find surprisingly that the insertion of the SrTiO$_3$ layer has increased the energy well depth and the effective barrier height for each stable state, even for the P_- state. This may indicate that the screening of the depolarization field may actually be enhanced by the presence of the SrTiO$_3$.

We would like to emphasize the fact that the enhanced ferroelectric properties of the heterostructure are obtained by replacing two layers of a *ferroelectric* BaTiO$_3$ by a *paraelectric* SrTiO$_3$. Given the fact that SrTiO$_3$ is unstrained

in the system considered, the ferroelectric polarization of the SrTiO₃ is not due to strain but induced by the adjacent BaTiO₃ layer. The overall enhancement of ferroelectric properties of the heterostructure results from elimination of the unfavorable interface termination. This behavior is different from the enhanced ferroelectricity found in layered ferroelectric/paraelectric heterostructures induced by strain.[44,45]

Our calculations for a thinner SrTiO₃ layer of one unit cell thickness predict similar behavior: changing the interface termination from BaO/RuO₂ to TiO₂/SrO results in dramatic enhancement of ferroelectric properties and leads to switchable polarization for thinner BaTiO₃ layers. We note that the system with one unit cell SrTiO₃ at the BaO/RuO₂ interface is identical to a system where BaTiO₃ layer has the TiO₂ termination at the two interfaces. Finally, our calculations for a SrTiO₃ layer deposited at the SrO/TiO₂ interface, i.e., the SrRuO₃/[SrTiO₃]₂[BaTiO₃]ₙ₋₂/SrRuO₃ heterostructure, do not predict enhanced ferroelectric properties. This result is expected due to the unfavorable BaO/RuO₂ termination remaining in this system.

III. PHENOMENOLOGICAL MODEL OF POLARIZATION STABILITY

A. Stability of SrRuO₃/[BaTiO₃]ₙ/SrRuO₃ at finite temperatures

To obtain further insight into the effect of interfaces on ferroelectric polarization stability and to explore this effect at finite temperatures we employ a phenomenological model developed by Gerra *et al.*[34] This model is based on the Ginzburg-Landau theory of ferroelectrics applied to thin films[46] that includes explicitly the term which depends on the interface polarization.[47,48] We consider a short-circuited ferroelectric film sandwiched between two electrodes. The Landau free energy includes a bulk term proportional to the film thickness and interface terms which are assumed to be different for the two interfaces. Specifically, for the SrRuO₃/BaTiO₃/SrRuO₃ heterostructure with asymmetric interfaces SrO/TiO₂ and RuO₂/BaO, the free energy Φ per unit surface area of the ferroelectric for two polarization states, P_+ and P_-, is given by equations

$$\Phi(P_+) = (A_0 P_+^2 + B P_+^4)h_{\text{BTO}} + X_+ P_+^2 + C P_+$$
$$\Phi(P_-) = (A_0 P_-^2 + B P_-^4)h_{\text{BTO}} + X_- P_-^2 + C P_-. \quad (3)$$

Here A_0 and B are parameters determined by the bulk properties of BaTiO₃, and h_{BTO} is the BaTiO₃ layer thickness corresponding to n unit cells of BaTiO₃. The parameters $X_\pm$ and C correspond to interface contributions to the free energy, so that $X_\pm = \eta_1 + \eta_2 + \lambda_\pm/\varepsilon_0$ and $C = \Delta\varphi_2 - \Delta\varphi_1 + \zeta_1 - \zeta_2$. Here $\zeta_{1,2}$ and $\eta_{1,2}$ are first- and second-order coefficients in the Taylor expansion of the free energy in terms of P near interfaces (indices 1 and 2 denote left and right interfaces); $\lambda_\pm = (\lambda_1^\pm + \lambda_2^\pm)/2$, where $\lambda_1^\pm$ and $\lambda_2^\pm$ are the effective screening lengths of the two interfaces corresponding to $P_\pm$; and $\Delta\varphi_1$ and $\Delta\varphi_2$ are work function steps at the two interfaces, as defined in Refs. 34 and 49. $\Delta\varphi_{1,2}$ and $\zeta_{1,2}$ are independent of the direction of P, and therefore C is chosen the same for both polarizations. By fitting the energy of bulk BaTiO₃ with in plane strain corresponding to the lattice constant of

SrTiO₃ as a function of ferroelectric displacements we find $A_0 = -1.318 \cdot 10^9$ C⁻²m²N and $B = 6.071 \cdot 10^9$ C⁻⁴m⁶N. By fitting the $n = 8$ energy data in Fig. 1(c) to Eq. (3) we find the surface parameters $C = 0.11$V, $X_+ = 1.437$ m²/F, and $X_- = 1.966$ m²/F, consistent with the respective parameters reported for the identical system in Ref. 34. Using these parameters we find that the phenomenological model is able to describe almost perfectly our first-principles results not only for the $n = 8$ structure but also for the thinner $n = 6$, 5, and 4 structures, as is seen from the dashed curves in Fig. 1(c). Therefore, the phenomenological model, combined with first-principles calculations, is effective to study ferroelectricity of the heterostructures considered in our work.

The calculations presented so far have assumed zero temperature. In the spirit of the Ginzburg-Landau approach, however, finite temperatures can be taken into account by replacing the quadratic parameter A_0 of the bulk with $A = A_0(T_c - T)/T_c$, where $T_c = 900$ K is an approximate ferroelectric transition temperature of BaTiO₃ under ~2% compressive strain as on SrTiO₃.[50,51] Assuming room temperature, $T = 300$ K, we can therefore predict the thickness dependence of ferroelectric stability of the SrRuO₃/[BaTiO₃]ₙ/SrRuO₃ heterostructures even for larger thicknesses, as plotted in Fig. 3(a). The interface effect caused by the built-in dipole is still present, as demonstrated by the fact that the double-well potential is asymmetric and that the P_+ state is less stable than the P_- state.

To estimate the critical thickness for the stability of the P_+ state, and therefore a switchable ferroelectric state, we employ the following criteria to these energy profiles: (i) an energy minimum with $P > 0$ must exist; (ii) if an energy minimum does exist for $P > 0$, such a minimum is only considered stable if the energy minimum is less than -4 meV/Ti, i.e., only if the well depth is larger than 4 meV/Ti. This second criterion stems from the fact that the energy profiles in Figs. 2 and 3 correspond to the restricted reversal path discussed in Sec. II.C. Since we find in Fig. 1(c) that the well depth of the $n = 6$ structure is apparently ~4 meV along this path but is not in fact stable when taking into account the possibility of a non-uniform polarization (as is true in the first-principles relaxation), we estimate that the well depth for reversal along our restricted path is overestimated by the same amount, 4 meV. Applying these criteria to the energy profiles at $T = 300$ K in Fig. 3(a), we find that when the BaTiO₃ thickness is below a critical thickness of about 16 unit cells [dashed curves in Fig. 3(a)], the P_+ polarization state is no longer stable.

B. Stability of SrRuO₃/[BaTiO₃]ₙ₋₂[SrTiO₃]₂/SrRuO₃ at finite temperatures

The phenomenological modeling of the "interface engineered" structure with the SrTiO₃ layer inserted proceeds in a similar manner. The new termination on interface caused by SrTiO₃, however, must be carefully considered. Geometrically, this structure can be viewed as SrRuO₃/[BaTiO₃]₍ₙ₋₁.₅₎[SrTiO₃]₁.₅/SrRuO₃ with BaTiO₃ terminated by TiO₂ on both sides and one monolayer of SrO in SrTiO₃ can be viewed as part of SrRuO₃. Because we now have the same termination on both sides, the parameter which
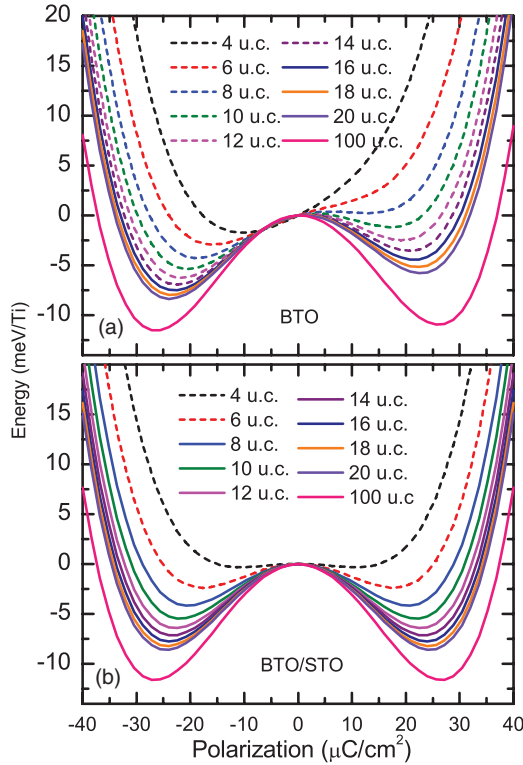
FIG. 3. (Color online) Free energy per Ti atom as a function of average polarization predicted by phenomenological modeling at finite temperature $T = 300$ K for (a) SrRuO$_3$/[BaTiO$_3$]$_n$/SrRuO$_3$ and (b) SrRuO$_3$/[BaTiO$_3$]$_{n-1.5}$[SrTiO$_3$]$_{1.5}$/SrRuO$_3$ structure with different numbers of titanate unit cells (u.c.), n. Solid curves correspond to those structures with both energy wells deeper than 4 meV/Ti, indicating switchable bi-stability according to the criteria described in Sec. III A. Dashed curves correspond to those structures with at least one energy well less than 4 meV deep, indicating the absence of switchability.

describes asymmetry can be considered negligible, i.e., $C \approx 0$. Based on our first-principles calculations predicting induced ferroelectric polarization in SrTiO$_3$, we introduce an additional term, $(A^* P_\pm^2 + B^* P_\pm^4)h_{STO}$, to the free energy to describe the SrTiO$_3$ interlayer. Taking all the above into account, we modify Eq. (3) as follows:

$$\Phi(P_+) = (A P_+^2 + B P_+^4)h_{BTO} + X_+^* P_+^2$$
$$+ (A^* P_+^2 + B^* P_+^4)h_{STO}$$
$$\Phi(P_-) = (A P_-^2 + B P_-^4)h_{BTO} + X_-^* P_-^2$$
$$+ (A^* P_-^2 + B^* P_-^4)h_{STO}, \quad (4)$$

where now h_{BTO} is the BaTiO$_3$ layer thickness corresponding to $(n - 1.5)$ unit cells of BaTiO$_3$, h_{STO} is the SrTiO$_3$ layer thickness corresponding to 1.5 unit cells of SrTiO$_3$, and $X_\pm^* = \eta_1^* + \eta_2^* + \lambda_\pm^*/\varepsilon_0$ are the new interface parameters. Just as in the case of the pure BaTiO$_3$ system, the additional parameters are obtained by fitting the energy data in Fig. 2(c) for the $n = 8$ SrRuO$_3$/[BaTiO$_3$]$_{n-1.5}$[SrTiO$_3$]$_{1.5}$/SrRuO$_3$ heterostructure. In this process, however, due to the accuracy of the polarization calculation, we simply assume that the spontaneous polarization $P_\pm$ of the system is the average polarization only within the 6 BaTiO$_3$ unit cells. Fitting reveals

that $(A^* h_{STO} + X_+^*) = 1.156$ m^2/F, $(A^* h_{STO} + X_-^*) = 1.173$ m^2/F, and $B^* = 7.571 \cdot 10^9$ C^{-4}m^{6}N.

Calculations for other thicknesses of BaTiO$_3$ are performed using the previous parameters fixed and only n being varied. We find that at zero temperature the phenomenological expression, Eq. (4), matches the first-principles calculations very well, as is evident from Fig. 2(c). To consider the effect of finite temperatures we include temperature dependence in the quadratic bulk term for bulk BaTiO$_3$ as we did for the system without the SrTiO$_3$ interlayer. The results are shown in Fig. 3(b) for room temperature and indicate the enhanced ferroelectric stability of the interface engineered system. With the substitution of two unit cells of BaTiO$_3$ by SrTiO$_3$, the critical thickness (determined by the same criteria described in Sec. III.A) with stable and switchable ferroelectric polarization is reduced by a factor of 2 from the system without SrTiO$_3$, demonstrating clear bi-stability down to an $n = 8$ unit-cell structure. This is apparent from Fig. 3(b) where solid and dashed lines distinguish stable and unstable polarization states.

C. Comments on stability against the formation of domains

In addition to the stability of a nonzero polarization in a uniformly polarized film, the stability of the monodomain state itself must be questioned. Below a certain critical thickness, which is generally larger than the critical thickness for the existence of a nonzero and switchable *local* polarization (as we have explored previously), the polarization profile of the film may break up into 180° domains with zero average polarization.[18–24] Such a polydomain state is unswitchable and therefore deleterious for applications. The question arises as to how the asymmetry of interfaces affects the critical thickness for the formation of a polydomain state. While a first-principles approach has previously been applied to explore a polydomain state,[23] finding the critical thickness for such a transition to occur is a daunting task due to the prohibitively large requirements on the size of the supercell. Instead, the problem is generally more tenable in terms of the phenomenological theory of ferroelectricity. Such a theoretical approach has been developed by Pertsev and Kohlstedt,[22] where the possibility of asymmetric interfaces can be incorporated in a straightforward fashion. While a detailed analysis of the interface dipole effect on domain formation is beyond the scope of this paper, a qualitative description is easy to formulate in terms of the structures we study here. A monodomain, uniform, polarization state has a propensity to lower its electrostatic energy due to the depolarizing field by forming domains. In the case of asymmetric interface, the parameter C, described in Sec. III.A, will effectively contribute a term to the depolarizing field of the form $-C/t$, independent of the polarization direction. In the case of the P_+ state, this contribution will effectively increase the depolarizing field, thereby increasing the critical thickness required for a stable and switchable monodomain state. Preliminary phenomenological modeling based on the theory developed by Pertsev and Kohlstedt[22] does indeed agree with this qualitative prediction, and further analysis will remain as the subject of a future study.

IV. SUMMARY AND CONCLUSIONS

In conclusion, based on the first-principles calculations and phenomenological modeling, we have established the importance of interface termination effects on ferroelectric stability of ultrathin $BaTiO_3$ films with $SrRuO_3$ electrodes. We showed that the presence of the BaO/RuO_2 termination sequence is detrimental to the switchable ferroelectric polarization due to an associated built-in interface dipole. This interface dipole points in the direction from the interface to the $BaTiO_3$ layer and, for thin $BaTiO_3$ layers, can completely suppress one polarization state, thereby making the system unswitchable and thus nonferroelectric. As a mechanism to alleviate this effect we demonstrate that ferroelectricity can be stabilized by replacing one or two unit cells of $BaTiO_3$ with $SrTiO_3$ at this interface, which essentially removes the detrimental interface dipole due to the BaO/RuO_2 termination in favor of the more stabilizing TiO_2/SrO interface. This method of alleviating unfavorable interface structures should be an efficient route to realize stable and switchable polarization in ferroelectric thin film heterostructures.

*jdburton1@gmail.com

†tsymbal@unl.edu

[1] J. F. Scott, *Ferroelectric Memories* (Springer, Germany, 2000).

[2] T. M. Shaw, S. Trolier-McKinstry, and P. C. McIntyre, Ann. Rev. Mater. Sci. **30**, 263 (2000).

[3] C. H. Ahn, K. M. Rabe, and J.-M. Triscone, Science **303**, 488 (2004).

[4] E. Y. Tsymbal and H. Kohlstedt, Science **313**, 181 (2006).

[5] M. Ye. Zhuravlev, R. F. Sabirianov, S. S. Jaswal, and E. Y. Tsymbal, Phys. Rev. Lett. **94**, 246802 (2005); **102**, 169901(E) (2009).

[6] H. Kohlstedt, N. A. Pertsev, J. Rodríguez-Contreras, and R. Waser, Phys. Rev. B **72**, 125341 (2005).

[7] V. Garcia, S. Fusil, K. Bouzehouane, S. Enouz-Vedrenne, N. D. Mathur, A. Barthelemy, and M. Bibes, Nature **460**, 81 (2009).

[8] A. Gruverman, D. Wu, H. Lu, Y. Wang, H. W. Jang, C. M. Folkman, M. Y. Zhuravlev, D. Felker, M. Rzchowski, C. B. Eom, and E. Y. Tsymbal, Nano Lett. **9**, 3539 (2009).

[9] M. Y. Zhuravlev, S. S. Jaswal, E. Y. Tsymbal, and R. F. Sabirianov, Appl. Phys. Lett. **87**, 222114 (2005).

[10] J. P. Velev, C.-G. Duan, J. D. Burton, A. Smogunov, M. K. Niranjan, E. Tosatti, S. S. Jaswal, and E. Y. Tsymbal, Nano Lett. **9**, 427 (2009).

[11] V. Garcia, M. Bibes, L. Bocher, S. Valencia, F. Kronast, A. Crassous, X. Moya, S. Enouz-Vedrenne, A. Gloter, D. Imhoff, C. Deranlot, N. D. Mathur, S. Fusil, K. Bouzehouane, and A. Barthelemy, Science **327**, 1106 (2010).

[12] M. Hambe, A. Petraru, N. A. Pertsev, P. Munroe, V. Nagarajan, and H. Kohlstedt, Adv. Func. Mater. **20**, 2436 (2010).

[13] J. D. Burton and E. Y. Tsymbal, Phys. Rev. Lett. **106**, 157203 (2011).

[14] S. Valencia, A. Crassous, L. Bocher, V. Garcia, X. Moya, R. O. Cherifi, C. Deranlot, K. Bouzehouane, S. Fusil, A. Zobelli, A. Gloter, N. D. Mathur, A. Gaupp, R. Abrudan, F. Radu, A. Barthélémy, and M. Bibes, Nat. Mater. **10**, 753 (2011).

[15] J. Junquera and P. Ghosez, Nature **422**, 506 (2003).

[16] C. Lichtensteiger, J.-M. Triscone, J. Junquera, and P. Ghosez, Phys. Rev. Lett. **94**, 047603 (2005).

[17] D. D. Fong, A. M. Kolpak, J. A. Eastman, S. K. Streiffer, P. H. Fuoss, G. B. Stephenson, C. Thompson, D. M. Kim, K. J. Choi, C. B. Eom, I. Grinberg, and A. M. Rappe, Phys. Rev. Lett. **96**, 127601 (2006).

[18] S. K. Streiffer, J. A. Eastman, D. D. Fong, C. Thompson, A. Munkholm, M. V. Ramana Murty, O. Auciello, G. R. Bai, and G. B. Stephenson, Phys. Rev. Lett. **89**, 067601 (2002).

[19] D. D. Fong, G. B. Stephenson, S. K. Streiffer, J. A. Eastman, O. Auciello, P. H. Fuoss, and C. Thompson, Science **304**, 1650 (2004).

[20] I. Kornev, H. Fu, and L. Bellaiche, Phys. Rev. Lett. **93**, 196104 (2004).

[21] B.-K. Lai, I. Ponomareva, I. I. Naumov, I. Kornev, H. Fu, L. Bellaiche, and G. J. Salamo, Phys. Rev. Lett. **96**, 137602 (2006).

[22] N. A. Pertsev and H. Kohlstedt, Phys. Rev. Lett. **98**, 257603 (2007).

[23] P. Aguado-Puente and J. Junquera, Phys. Rev. Lett. **100**, 177601 (2008).

[24] V. Nagarajan, J. Junquera, J. Q. He, C. L. Jia, R. Waser, K. Lee, Y. K. Kim, S. Baik, T. Zhao, R. Ramesh, Ph. Ghosez, and K. M. Rabe, J. Appl. Phys. **100**, 051609 (2006).

[25] D. J. Kim, J. Y. Jo, Y. S. Kim, Y. J. Chang, J. S. Lee, J.-G. Yoon, T. K. Song, and T. W. Noh, Phys. Rev. Lett. **95**, 237602 (2005).

[26] G. Gerra, A. K. Tagantsev, N. Setter, and K. Parlinski, Phys. Rev. Lett. **96**, 107603 (2006).

[27] A. K. Tagantsev and G. Gerra, J. Appl. Phys. **100**, 051607 (2006).

[28] Y. Umeno, J. M. Albina, B. Meyer, and C. Elsässer, Phys. Rev. B **80**, 205122 (2009).

[29] C.-G. Duan, R. F. Sabirianov, W.-N. Mei, S. S. Jaswal, and E. Y. Tsymbal, Nano Lett. **6**, 483 (2006).

[30] M. Stengel, D. Vanderbilt, and N. A. Spaldin, Nat. Mater. **8**, 392 (2009).

[31] H. Lu, X. Liu, C.-W. Bark, J. D. Burton, Y. Wang, Y. Zhang, D. J. Kim, A. Stamm, P. Lukashev, D. A. Felker, C. M. Folkman, P. Gao, X. Q. Pan, M. S. Rzchowski, C.-B. Eom, E. Y. Tsymbal, and A. Gruverman, Adv. Mater. **24**, 1209 (2012).

[32] G. Kresse and J. Furthmüller, Comput. Mater. Sci. **6**, 15 (1996).

[33] S. J. May, J. W. Kim, J. M. Rondinelli, E. Karapetrova, N. A. Spaldin, A. Bhattacharya, and P. J. Ryan, Phys. Rev. B **82**, 014110 (2010).

[34] G. Gerra, A. K. Tagantsev, and N. Setter, Phys. Rev. Lett. **98**, 207601 (2007).

[35] J. M. Rondinelli, M. Stengel, and N. A. Spaldin, Nature Nano. **3**, 46 (2008).

[36] J. D. Burton and E. Y. Tsymbal, Phys. Rev. B **82**, 161407 (2010).

[37] H. J. Chang, S. V. Kalinin, A. N. Morozovska, M. Huijben, Y.-H. Chu, P. Yu, R. Ramesh, E. A. Eliseev, G. S. Svechnikov, S. J. Pennycook, and A. Y. Borisevich, Adv. Mater. **23**, 2474 (2011).

[38] C.-Q. Jin, J.-S. Zhou, J. B. Goodenough, Q. Q. Liu, J. G. Zhao, L. X. Yang, Y. Yu, R. C. Yu, T. Katsura, A. Shatskiy, and E. Ito, Proc. Natl. Acad. Sci. **105**, 7115 (2008).

[39] Y. Wang, M. K. Niranjan, K. Janicka, J. P. Velev, M. Ye. Zhuravlev, S. S. Jaswal, and E. Y. Tsymbal, Phys. Rev. B **82**, 094114 (2010).

[40] R. M. Pick, M. H. Cohen, and R. M. Martin, Phys. Rev. B **1**, 910 (1970).

[41] We note that the method based on the Born effective charges calculated for bulk ferroelectrics cannot provide a quantitatively accurate description of the local polarization distribution in heterostructures due to the effects of interfaces and local fields which do not exist in the bulk. Nevertheless, we find this approach valuable for a semiquantitative exploration of the polarization behavior.

[42] K. M. Rabe, C. H. Ahn, and J.-M. Triscone, *Physics of Ferroelectrics—A Modern Perspective* (Springer, Germany, 2007).

[43] R. D. King-Smith and D. Vanderbilt, Phys. Rev. B **47**, 1651 (1993).

[44] H. N. Lee, H. M. Christen, M. F. Chisholm, C. M. Rouleau, and D. H. Lowndes, Nature **433**, 395 (2005).

[45] S. M. Nakhmanson, K. M. Rabe, and D. Vanderbilt, Phys. Rev. B **73**, 060101 (2006).

[46] R. Kretschmer and K. Binder, Phys. Rev. B **20**, 1065 (1979).

[47] M. D. Glinchuk and A. N. Morozovska, J. Phys. Condens. Matter **16**, 3517 (2004).

[48] A. M. Bratkovsky and A. P. Levanyuk, Phys. Rev. Lett. **94**, 107601 (2005).

[49] A. K. Tagantsev, G. Gerra, and N. Setter, Phys. Rev. B **77**, 174111 (2008).

[50] N. A. Pertsev, A. G. Zembilgotov, and A. K. Tagantsev, Phys. Rev. Lett. **80**, 1988 (1998).

[51] K. J. Choi, M. Biegalski, Y. L. Li, A. Sharan, J. Schubert, R. Uecker, P. Reiche, Y. B. Chen, X. Q. Pan, V. Gopalan, L. Q. Chen, D. G. Schlom, and C. B. Eom, Science **306**, 1005 (2004).